N84-34897

"GROUND-BASED OBSERVATIONS OF EQUATORIAL THERMOSPHERE DYNAMICS WITH A FABRY-PEROT INTERFEROMETER"

Final Report

Principal Investigator:

John W. Meriwether, Jr.
Space Physics Research Laboratory
The University of Michigan
Ann Arbor, Michigan 48109-2143

and

Co-Author:

Manfred A. Biondi
Physics Astronomy Department
University of Pittsburgh
Pittsburgh, Penna. 45260

Period Covered:

December 1, 1982 thru
September 30, 1984

Space Physics Research Laboratory
The University of Michigan
Ann Arbor, Michigan 48109-2143

NASA GRANT NAG 5-615

The funding provided in this grant supported the installation of a Fabry-Perot Interferometer at the site of Arequipa, Peru. Measurements were made throughout the year to assess thermospheric winds and temperatures for an equatorial location. Appendix A reports on the analysis of the temperature data, with a comparison of the MSIS model for quiet and active magnetic periods, and for low and moderate levels of solar activity. Appendix B presents the results of thermospheric wind observations throughout the same period. The chosen site of Arequipa, Peru is well suited to these observations because of the excellent seeing conditions, and the availability of high quality engineering support provided by the NASA lidar facility staff at this site.

Although it was hoped that thermosperic winds and temperature measurements could be made during the period of Project Condor in early March, 1983, this was not possible. The instrument was perational at Arequipa at the time requested, but cloud cover conditions prohibited any useful measurements. Some clear skies became available by mid-March, however, the full moon conditions during this time rendered the observations useless because of the high background associated with the lunar illumination. The best measurements came during the dark moon periods of the following months beginning with April, 1983. Measurements were terminated in mid-August due to equipment problems caused by damage of the power invertor required to convert 50 hertz to 60 hertz frequency. These problems have been remedied and the observatory is currently in operation at this time.

Appendix A has been submitted to the Geophysical Research Journal for publication. The figures in the Appendix B were presented at the Thermospheric Dynamics workshop meeting at Calverton, Maryland, on the 4th of October, 1984. This material will form the basis for a publication in GRL.

4L63.46W

APPENDIX A

MEASURED RESPONSE OF THE EQUATORIAL THERMOSPHERIC TEMPERATURE TO GEOMAGNETIC ACTIVITY AND SOLAR FLUX CHANGES

Manfred A. Biondi
Dept. of Physics and Astronomy
University of Pittsburgh, Pittsburgh, PA 15260

and

John W. Meriwether, Jr.
Space Physics Research Laboratory
University of Michigan, Ann Arbor, MI 48109

Abstract - Fabry-Perot determinations of thermospheric temperatures from 630.0 nm nightglow line width measurements have been carried out for the period April-August 1983 from Arequipa, Peru (16.5°S, 71.5°W geographic; 5°S magnetic). The nightly variation of the thermospheric temperature T_n measured on 53 nights is compared with MSIS model predictions and found to agree occasionally with the model but, on average, to exceed model predictions by $\sim$ 180 K. The largest differences, 400-500 K, occur during strongly increasing geomagnetic activity such as sudden commencements. Significant differences occur both during high geomagnetic/low solar activity and during low geomagnetic/high solar activity. A suggested origin of the rapid increase in T_n which follows sudden increases in geomagnetic activity with $\lesssim$ 1 day delay is the energy carried to equatorial regions from high-latitude (auroral oval) heat sources at both poles by gravity waves and equatorward neutral winds.

Introduction

The temperature of the neutral thermosphere has been monitored by various ground-based and satellite techniques which include direct determinations such as measurements of the doppler width of the 630.0 nm airglow line and indirect methods such as radar backscatter plasma measurements and satellite orbit decay observations (see, for example, Jacchia, 1977; Hedin et al, 1977; Thuillier et al, 1977; Hernandez, 1982; Sipler et al, 1983 and the references cited therein). The temperature is expected to change in response to changing energy inputs in the heat balance equation governing the neutral thermosphere, in particular, to changes in the fluxes of solar radiation and of precipitating particles which are stopped in the upper atmosphere. A number of semi-empirical models (e.g., Jacchia, 1977; Hedin et al, 1977; Thuillier et al, 1977) which predict thermospheric temperatures on the basis of indices related to solar euv and high-latitude precipitating particle fluxes, e.g. $F_{10.7}$, K_p or A_p, etc., appear to provide reasonable agreement with measured nightly mean temperatures at mid-latitude (Hernandez, 1982); however, the measured diurnal variations and responses during geomagnetic storm conditions often are rather different from the predicted behavior.

Recently, an automated airglow observatory has been set up at Arequipa, Peru (16.5°S, 71.5°W geographic, 5°S geomagnetic) in a joint effort by the Universities of Pittsburgh and Michigan, with the cooperation of the personnel of the NASA Laser Satellite Tracking Station at Arequipa. The principal observatory instrument is a field-widened 100 mm aperture Fabry-Perot interferometer suitable for nightglow 630.0 nm doppler width and doppler shift determinations. The unusually clear weather at Arequipa permits nightglow measurements on many successive nights (the limitation in data-taking to date has largely been due to apparatus problems engendered by power line transients and the pervasive, fine dust carried by daytime winds). Thus, it has been possible to obtain sequences of $\sim$ 12 hour measurements of nightime temperatures to investigate the short-term response of the thermosphere to changing solar euv radiation and geomagnetic activity.

The present paper details measurements of the neutral temperature in the equatorial thermosphere over Arequipa for the period 1 April - 9 August 1983, during which some 90 nights of useful data were obtained, 53 of which have been reduced, and compares them with changes in solar flux and geomagnetic activity indices on both short- (few hour) and longer-term (weeks) time scales.

Apparatus

The optical apparatus and its electronic control hardware are very similar to those described in detail by Sipler et al (1983), while the computer control and data acquisition system and its software are of the type described by Meriwether et al (1983); therefore only a brief description will be given here. The system provides for automatic observations of the 630.0 nm nightglow line by the Fabry-Perot interferometer and a companion tilting filter photometer. The common lines-of-sight of the two instruments are directed to the desired point in the sky by a two-axis, stepping-motor-driven pointing head on the roof of the observatory building.

The tilting filter photometer monitors the wavelength range 628-631 nm in order to detect interfering radiation (e.g., from OH) and cloud effects on the 630.0 nm observations.

The 100 mm aperture Fabry-Perot (F-P) is index-of-refraction tuned ("pressure-scanned") by changing the density of argon gas between the F-P plates with a stepping-motor-driven volume changer consisting of a piston and cylinder sealed by a rolling diaphragm. The F-P is field-widened by a multi-aperture exit plate which provides a gain of ∿ 3.8 in luminosity over a central aperture exit plate instrument. The 630.0 nm line profiles are obtained by coherently summing a number of wavelength scans across the line until either a predetermined signal level has been achieved or a maximum time interval has elapsed. After this, the computer directs the lines-of-sight of the instruments to the next observing position.

Radiation from a stabilized 632.8 nm helium-neon laser is periodically (at intervals ranging from 20 to 120 min) introduced to the F-P to provide a determination of the instrumental broadening function, which is accomplished by computer-fitting the 632.8 nm line profile with a 10-term Fourier series. This truncated series is convolved with a gaussian line shape (the assumed form of the nightglow emission) and then least-squares fitted to the measured 630.0 nm profiles to yield line center frequency, line width, integrated intensity and background (Wickwar et al, 1984). The estimated error in the neutral temperatures determined from the line widths varies with the 630.0 nm nightglow intensity, ranging from $\pm$ 30 K to $\pm$ 70 K in most cases.

Results

A summary of the neutral temperatures determined from the 630.0 nm doppler widths is presented in Fig. 1, together with published values of the solar flux (Sa) and geomagnetic planetary three-hour-range indices (K_p) from the World Data Center A for Solar-Terrestrial Physics. The nightly ($\sim$ 12 hour duration) determinations of T_n are indicated by the broad lines, most of whose width results from differences in temperature noted in different observing directions, e.g., N, E, S, W. The trend of the lines indicates a rough average of the change of temperature during the course of each night, some nights yielding a modest fall, as normally expected, others indicating a sharper fall or a fall followed by a rise. The short, narrow lines on the T_n plots are the MSIS model predictions (A. E. Hedin, private communication, 1984), using measured values of the solar and geomagnetic indices for the period shown.

In order to compare short-term response of T_n to changes in geomagnetic activity, detailed measurements on selected nights are shown in Fig. 2, with the symbols N, E, S, W indicating the observing azimuths (elevation = 30° in all cases). The solid lines are the MSIS model predictions. The sequence of six nights shown in Fig. 2 involves a period of smoothly falling solar flux but a change from geomagnetically quiet to disturbed back to quiet conditions. In passing, we note in the data of 4, 5, 6 August evidence of the post-midnight rise in T_n which has been observed at low and equatorial latitudes by a number of investigators, for example, by Spencer et al (1979).

Discussion and Conclusions

It is clear from Figs. 1 and 2 that, while there are some nights when the T_n values deduced from the 630.0 nm line width measurements agree reasonably with the MSIS model predictions, e.g., during August, many of the measurements yield temperatures significantly higher (100 K - 400 K) than the predicted values. Non-thermal broadening of the 630.0 nm nightglow line by sources such as remnants of the dissociation kinetic energy from the electron-ion recombination which produces the $O(^1D)$ atoms or kinetic energy of precipitating energetic oxygen atoms (Torr and Torr,

1984) can not account for the elevated temperatures measured. In the former case, complete slowing by collisions before radiation will occur at expected emission altitudes (< 400 km), while, in the latter, the relatively few energetic O atoms would have to share their kinetic energy with and simultaneously excite the ambient O atoms to the ^1D state in order to have a discernible effect near the doppler core of the line.

We have been unable to find any instrumental effect which can account for erroneously high temperatures of the required magnitude. For example, spurious broadening due to instrumental drifts during the long periods of scan summing required by weak airglow emission can not account for the effect, since high temperatures were measured during periods of both low and high 630.0 nm nightglow intensity. Also, errors in instrumental width determinations due to improper frequency locking of the stabilized He-Ne laser would lead to an underestimate, rather than an overestimate of the 630.0 nm line width and, therefore, of T_n.

Significant differences between measured T_n values and MSIS predictions occur both during periods of high solar/low geomagnetic activity, e.g., June 3-7 and during periods of low solar/high geomagnetic activity, e.g., April 1-16. Thus, the underestimate of the measured exospheric temperatures by the MSIS model can not be traced to an incorrect dependence on one activity index (solar or geomagnetic) alone.

Our measurements of equatorial thermospheric temperatures over Kwajalein Atoll during August and September 1977 (Sipler et al, 1983) also yielded higher values, on the average, (by $\sim$ 330 K) than the MSIS model predictions. In addition, Hernandez (1982) has analyzed the T_n values he obtained from 630.0 nm nightglow line width measurements at midlatitude (Fritz Peak Observatory, Colorado) from 1972 to 1979 and finds that his measured values exceed the MSIS model predictions by an average of 100-150 K. The measured values in Fig. 1 exceed the MSIS model predictions by ∿ 180 K on the average, so that substantial differences between values of T_n determined by ground-based FP's and those of the MSIS model (empirically derived by fitting satellite mass spectrometer and incoherent scatter data to solar and geomagnetic indices) seem to be a continuing problem at mid- and equatorial latitudes. These differences can not be traced to an inherent, large discrepancy between ground-based F-P and incoherent scatter determinations, since simultaneous F-P and backscatter determinations of T_n reported in two papers (Cogger et al, 1970 and Hernandez et al, 1975) revealed only a small difference, $\lesssim$ 30 K, for the T_n's determined by the two techniques.

In examining the short-term response ($\lesssim$ 1 day) of the thermospheric temperature to rather rapid changes in solar EUV flux or to energy inputs at high-latitudes from particle precipitation, etc., it is inappropriate to use semi-empirical models such as MSIS or those of Jacchia, which are intended to describe average or longer-term behavior. Indeed, our findings of rapid responses of T_n to strongly increased geomagnetic activity, especially sudden commencements, are not reflected in the MSIS model predictions for those periods (see, for example, the data of 2-3 August, 6-8 August, and possibly 12-13 June in Figs. 1 and 2). In these cases, when a sudden increase in K_p occurs, the measured T_n values remain low for up to a day and then increase sharply.

A partial explanation of these observations may be found in gravity wave propagation of energy from a high latitude heating source to low latitudes. For example, recent calculations by Mayr et al (1984) have indicated substantial elevation of exospheric temperatures at equatorial latitudes, $\Delta T_n/T_{no} \sim 0.2$, several hours after the onset of Joule heating in the northern auroral oval (in the region of the heat source, $[\Delta T_n/T_{no}]_{max} \sim 1$). Such efficient and rapid propagation of energy may well be the source of the occasional, rapid response of the low-latitude thermosphere to surges in high latitude heating. Also, equatorward winds driven by Joule heating in both the North and South auroral ovals and averaging 100-200 m/s would cause compressional heating of the equatorial thermosphere about a day after the onset. Fejer et al (1983) have attributed observed changes in the vertical drifts of the equatorial F-region over Jicamarca, Peru, which occur about one day after the onset of some geomagnetic storms, to similar changes in the thermospheric circulation pattern. These effects should be calculable by refinements of thermospheric general circulation models such as those of Dickinson et al (1981).

In summary, the present measurements at equatorial latitudes yield average nighttime thermospheric temperatures which are significantly higher than MSIS model predictions, a finding similar to that noted at midlatitude by Hernandez (1982). Further, the rapid ($\lesssim$ 1 day) and large response of T_n to sudden changes in geomagnetic indices suggests efficient and rapid transport of energy injected at high latitudes to the equatorial thermosphere, probably by gravity waves or by extensive, storm-generated equatorward winds.

Acknowledgements. The authors are indebted to J. Moody, who reduced the data tapes of the Arequipa observations, and to B. Kennedy, L. Slider, and C. Tepley, who contributed importantly to the set up of the observatory. Thanks are also due to NASA and to the Smithsonian Astrophysics Observatory for making available the observatory site at the Laser Satellite Tracking

Station and to the station personnel, particularly D. Hallenbeck and T. Muszynski, for their constant and continuing assistance in setting up and maintaining the apparatus. We are grateful to A. Hedin for providing the MSIS model predictions and to H. Mayr for making available the gravity wave results prior to publication. This research was supported, in part, by the Division of Atmospheric Sciences, National Science Foundation under Grant ATM-8121723 to the University of Pittsburgh and Grant ATM-8202440 to the University of Michigan and by NASA Grant NAG5-615 to the University of Michigan.

References

Dickinson, R. E., E. C. Ridley and R. G. Roble, A three-dimensional general circulations model of the thermosphere, J. Geophys. Res., 86, 1499-1512, 1981.

Fejer, B. G., M. F. Larsen and D. T. Farley, Equatorial disturbance dynamo electric fields, Geophys. Res. Letts., 10, 537-540, 1983.

Hedin, A. E., J. E. Salah, J. V. Evans, C. W. Reber, G. P. Newton, N. W. Spencer, D. C. Kayser, D. Alcayde, P. Bauer, L. L. Cogger and J. P. McClure, A global thermospheric model based on mass spectrometer and incoherent scatter data, MSIS 1. N_2 density and temperature, J. Geophys. Res., 82, 2139-2147, 1977.

Hernandez, G., Midlatitude thermospheric neutral kinetic temperatures 1. Solar, geomagnetic and long-term effects, J. Geophys. Res., 87, 1623-1632, 1982.

Jacchia, L. G., Thermospheric temperature, density and composition: New models, Spec. Rep. 375, Smithson. Astrophys. Obs., Cambridge, Mass., 1977.

Mayr, H. G., I. Harris, F. Varosi and F. A. Herrero, Global excitation of wave phenomena in a dissipative multiconstituent medium, submitted to J. Geophys. Res., 1984.

Meriwether, J. W., C. A. Tepley, S. A. Price, P. B. Hays and L. L. Cogger, Remote ground-based observations of terrestrial airglow emissions and thermospheric dynamics at Calgary, Alberta, Canada, Optical Engineering, 22, 128-131, 1983.

Sipler, D. P., M. A. Biondi and R. G. Roble, F-region neutral winds and temperatures at equatorial latitudes: Measured and predicted behavior during geomagnetically quiet conditions, Planet. Space Sci., 31, 53-66, 1983.

Spencer, N. W., G. R. Carignan, H. G. Mayr, H. B. Niemann, R. F. Theis, and L. E. Wharton, The midnight temperature maximum in the earth's equatorial thermosphere, Geophys. Res. Letts., 6, 444-446, 1979.

Thuiller, G., J. L. Falin and C. Wachtel, Experimental global model of the exospheric temperature based on measurements from the Fabry-Perot interferometer on board the OGO-6 satellite - discussion of the data and properties of the model, J. Atmos. Terr. Phys., 39, 399-414, 1977.

Torr, M. R. and D. G. Torr, Energetic oxygen in a mid-latitude aurora, J. Geophys. Res., 89, 5547-5553, 1984.

Wickwar, V., J. W. Meriwether, P. B. Hays and A. F. Nagy, The meridional thermospheric neutral wind measured by radar and optical techniques in the auroral region, J. Geophys. Res., 1984, in press.

Figure Captions

Fig. 1 Nighttime thermospheric temperatures T_n, geomagnetic planetary three-hour-range indices K_p and solar flux values Sa as a function of world date for March-August 1983. On the T_n graphs: broad curves - measured values in various directions; short, narrow lines - MSIS model predictions. The arrows on the K_p graphs indicate sudden commencements.

Fig. 2 Nighttime thermospheric temperatures during August, 1983 (00^h LT = 05^h UT). The three-hour K_p indices are given at the top of each graph. Measured temperatures in various directions: N, E, S, W symbols (the error bars, ranging from $\pm$ 30 K to $\pm$ 70 K, are omitted for clarity). MSIS model predictions: solid curves.

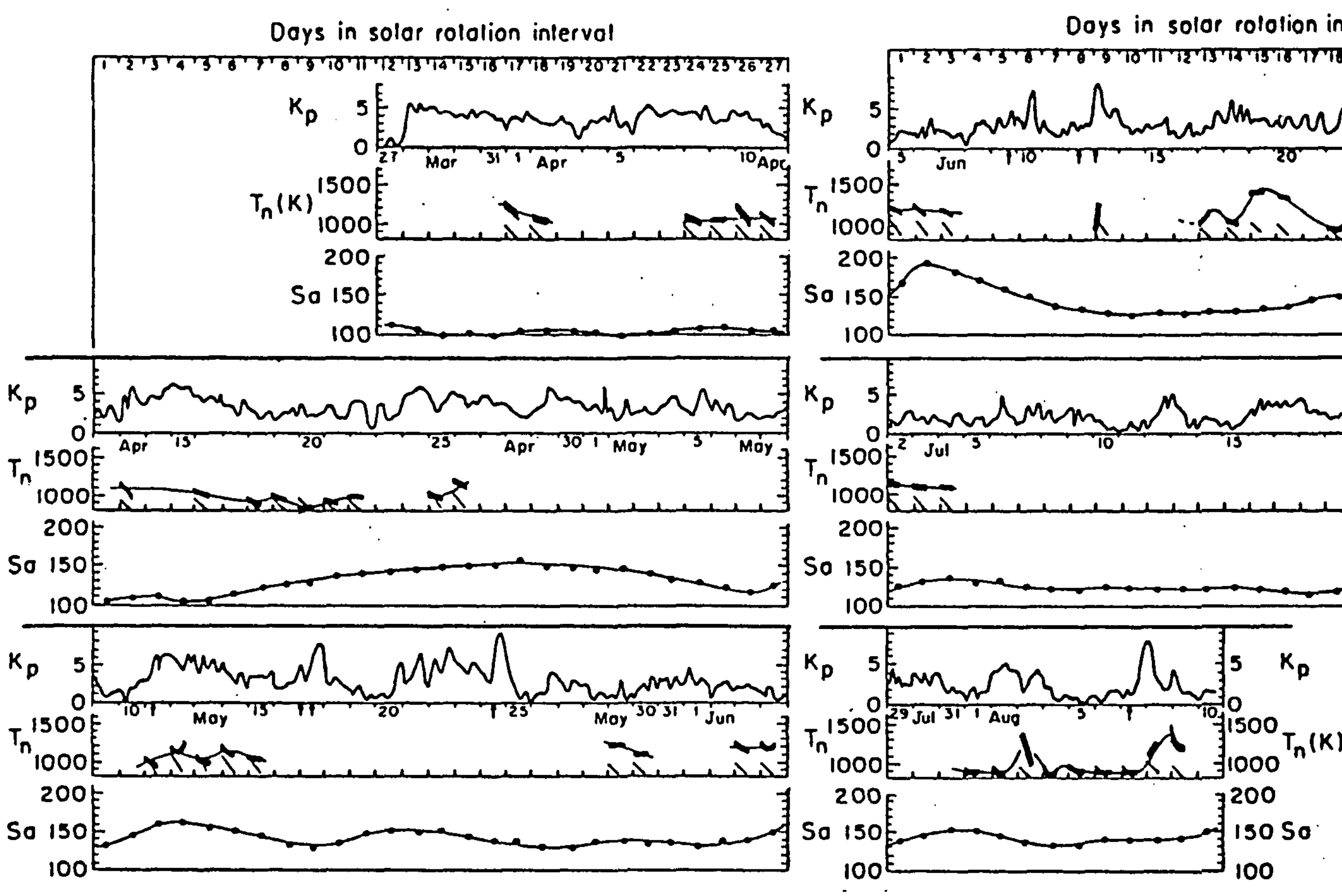

Days in solar rotation interval
Days in solar rotation interval
K_p
T_n(K)
Sa
Mar
Apr
May
Jun
Jul
Aug

Fig. 1

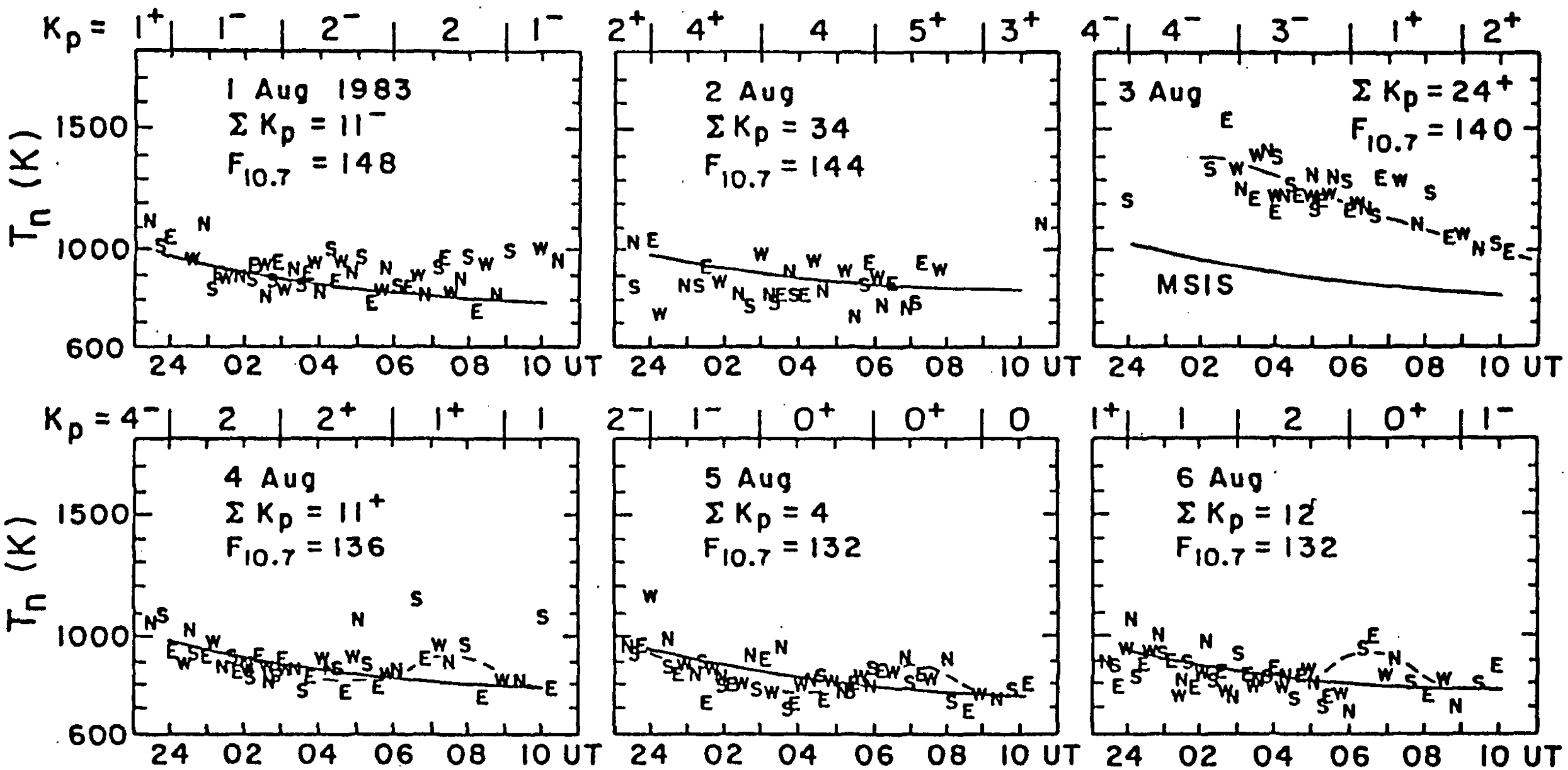

Kp = 1+ 1- 2- 2 1- 2+ 4+ 4 5+ 3+ 4- 4- 3- 1+ 2+
1 Aug 1983
Σ Kp = 11-
F10.7 = 148
2 Aug
Σ Kp = 34
F10.7 = 144
3 Aug
Σ Kp = 24+
F10.7 = 140
MSIS
Kp = 4- 2 2+ 1+ 1 2- 1- 0+ 0+ 0 1+ 1 2 0+ 1-
4 Aug
Σ Kp = 11+
F10.7 = 136
5 Aug
Σ Kp = 4
F10.7 = 132
6 Aug
Σ Kp = 12
F10.7 = 132
Tn (K)
1500
1000
600
24 02 04 06 08 10 UT

Fig. 2

APPENDIX B

Equatorial thermospheric measurements of temperatures and winds at Arequipa, Peru

John W. Meriwether, Jr.

Space Physics Research Laboratory
University of Michigan
Ann Arbor, Michigan

Manfred A. Biondi

Department of Physics
University of Pittsburgh
Pittsburgh, Pennsylvania

Arequipa FPI observatory: facts

* Field-widened 10 cm FPI
  Automatic operations

* Located at Arequipa, Peru (16.5S, 71.5W)
  (at the NASA lidar satellite tracking station)
  4.5 degrees south of magnetic equator
  FPI observes winds overhead of Jicamarca radar

* Observing directions typically
  Z,N,S,W or N,S,E,W

* Data selected from observations between
  new moon, April, 1983, and new moon,
  August, 1983; 55 nights reduced.
  Some results from 1984 but not all reduced.

* Error bars typically 15-20 m/s for winds,
  50 to 75 degrees for temperature

Equatorial kinetic temperature: Results

* Enhancement of FPI temperatures above quiet levels a few hours after the start of magnetic activity. Magnitude of this enhancement about 300 degrees. This is followed by relaxation to pre-storm levels.

* Apparent average offset of FPI temperatures from MSIS by 100-200 degrees for relatively quiet times.

* Definite suggestion of a midnight thermal enhancement for April and August data. Magnitude about 100 degrees. Seen in both 1983 and 1984 observatons.

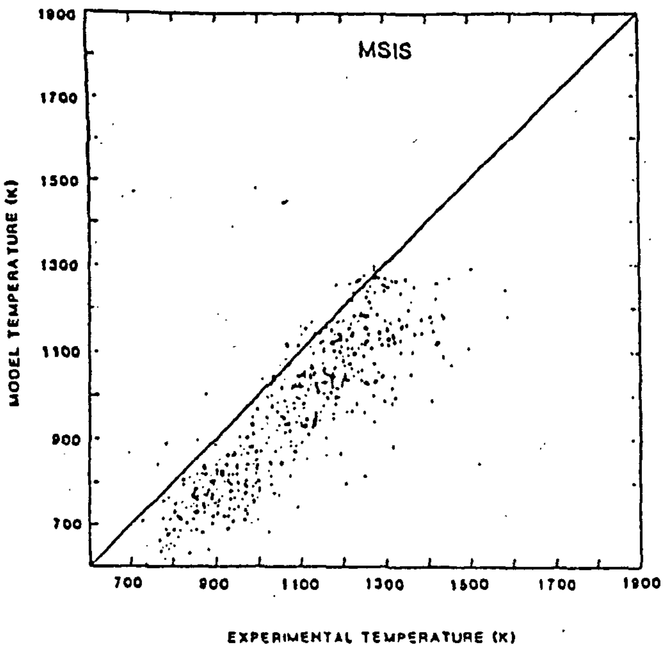

Fig. 3. Comparison of the experimental temperatures with the *MSIS* empirical model [*Hedin et al.*, 1977].

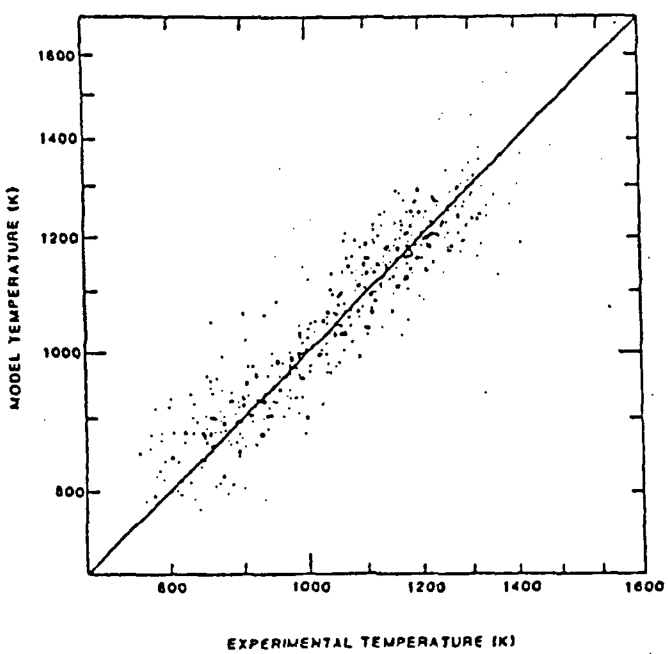

Fig. 11. Fit of the experimental data to four parameters: solar radio flux, geomagnetic activity, annual variation of the solar declination and a semi-annual variation. The correlation coefficient is 0.91.

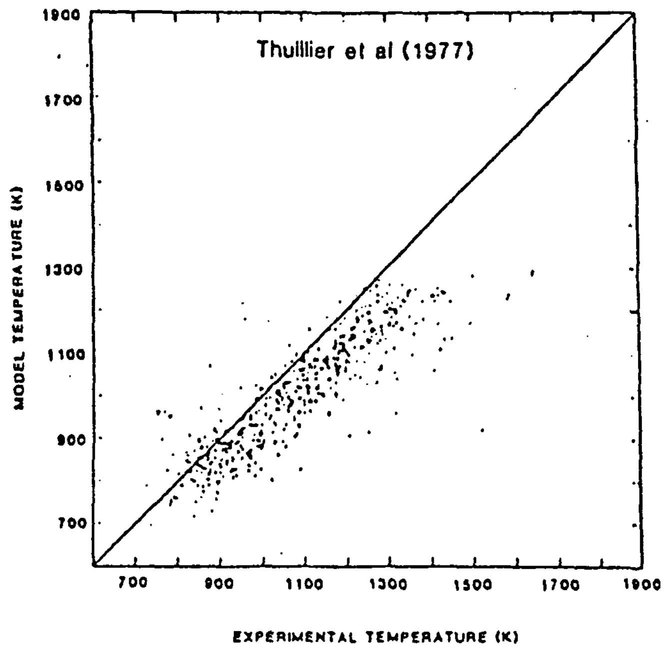

Fig. 4. Comparison of the experimental temperature with the empirical model of *Thuillier et al.* [1977*a*, *b*].

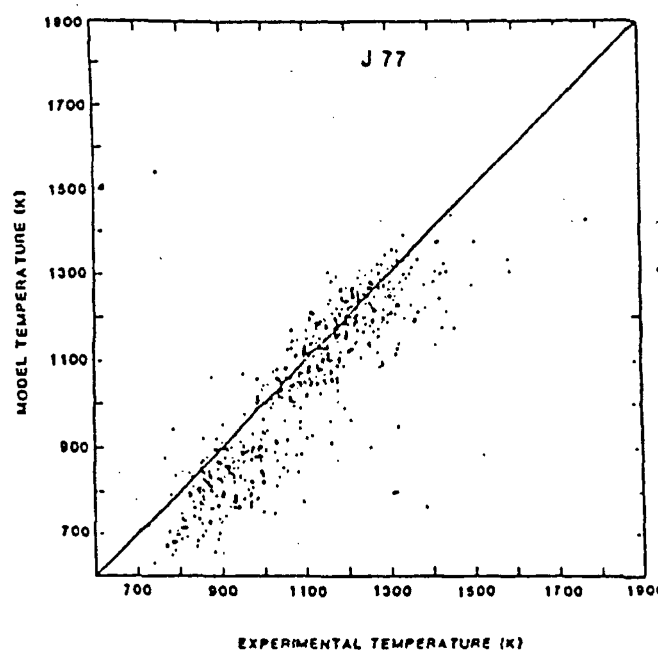

Fig. 5. Comparison of the experimental temperatures with the empirical model of *Jacchia* [1977].

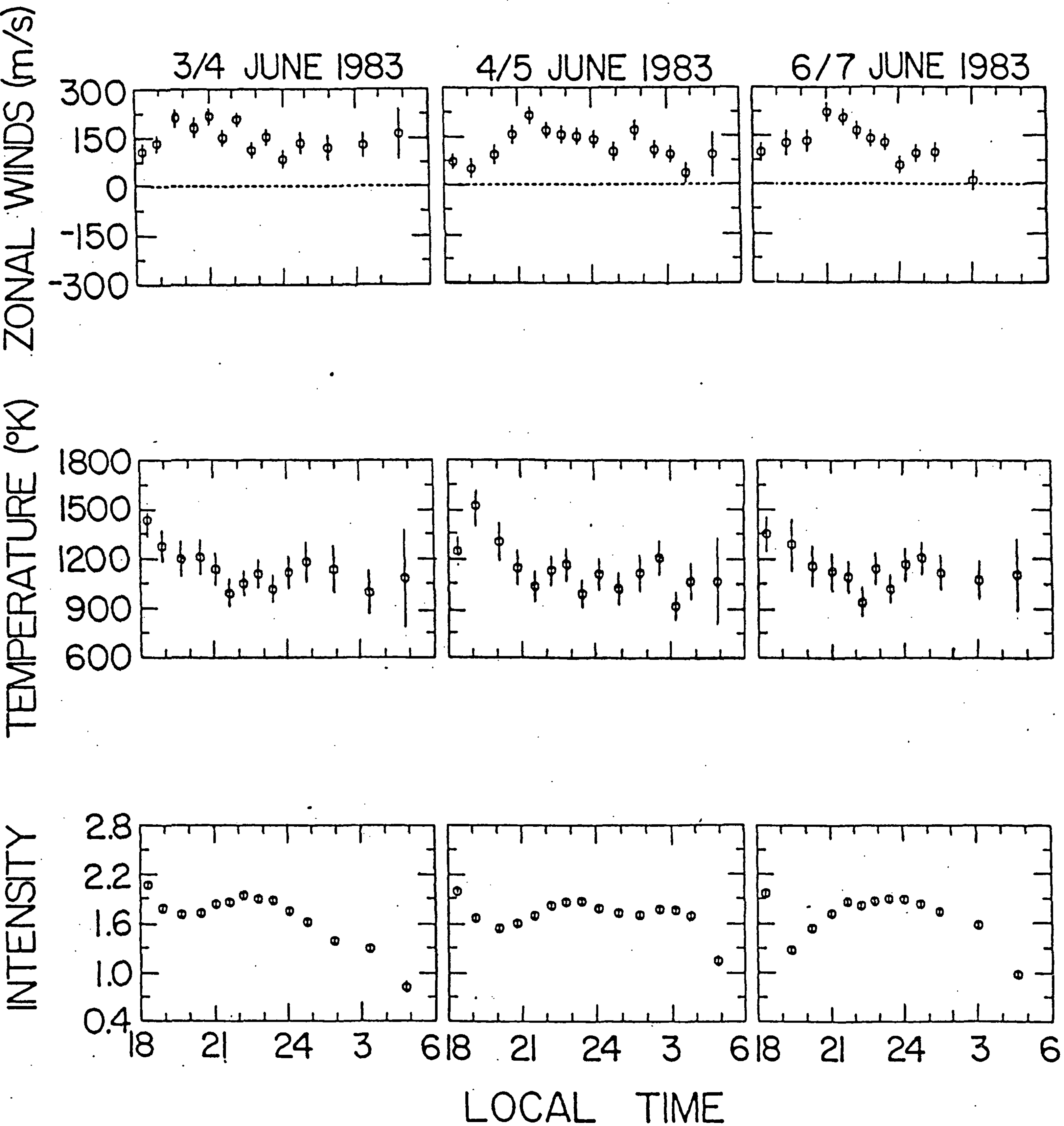

3/4 JUNE 1983
4/5 JUNE 1983
6/7 JUNE 1983
ZONAL WINDS (m/s)
300
150
0
-150
-300
TEMPERATURE (°K)
1800
1500
1200
900
600
INTENSITY
2.8
2.2
1.6
1.0
0.4
18
21
24
3
6
LOCAL TIME

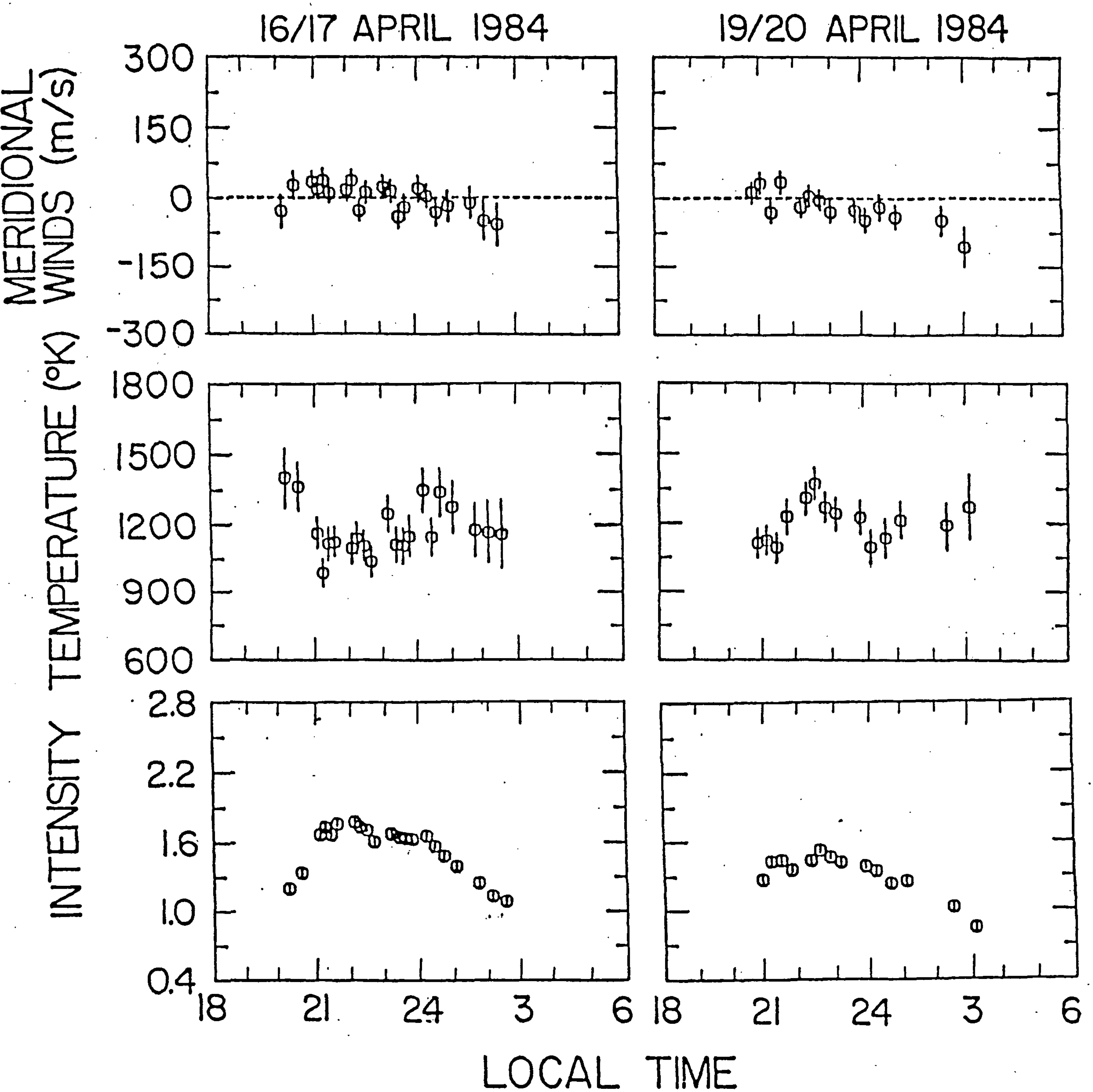

16/17 APRIL 1984
19/20 APRIL 1984
MERIDIONAL WINDS (m/s)
300
150
0
-150
-300
TEMPERATURE (°K)
1800
1500
1200
900
600
INTENSITY
2.8
2.2
1.6
1.0
0.4
18
21
24
3
6
LOCAL TIME

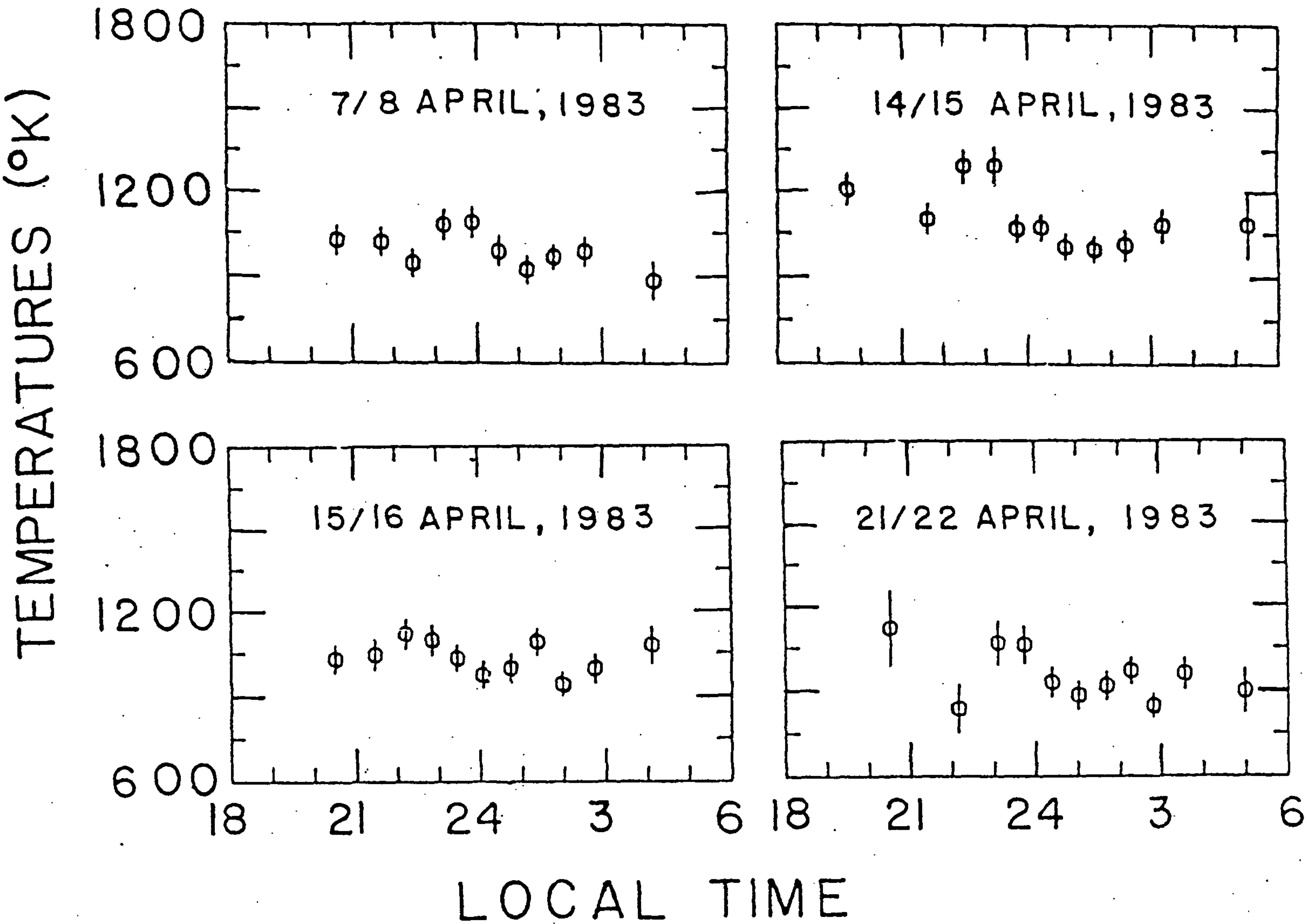
TEMPERATURES (°K)
1800
1200
600
7/8 APRIL, 1983
14/15 APRIL, 1983
15/16 APRIL, 1983
21/22 APRIL, 1983
18
21
24
3
6
LOCAL TIME

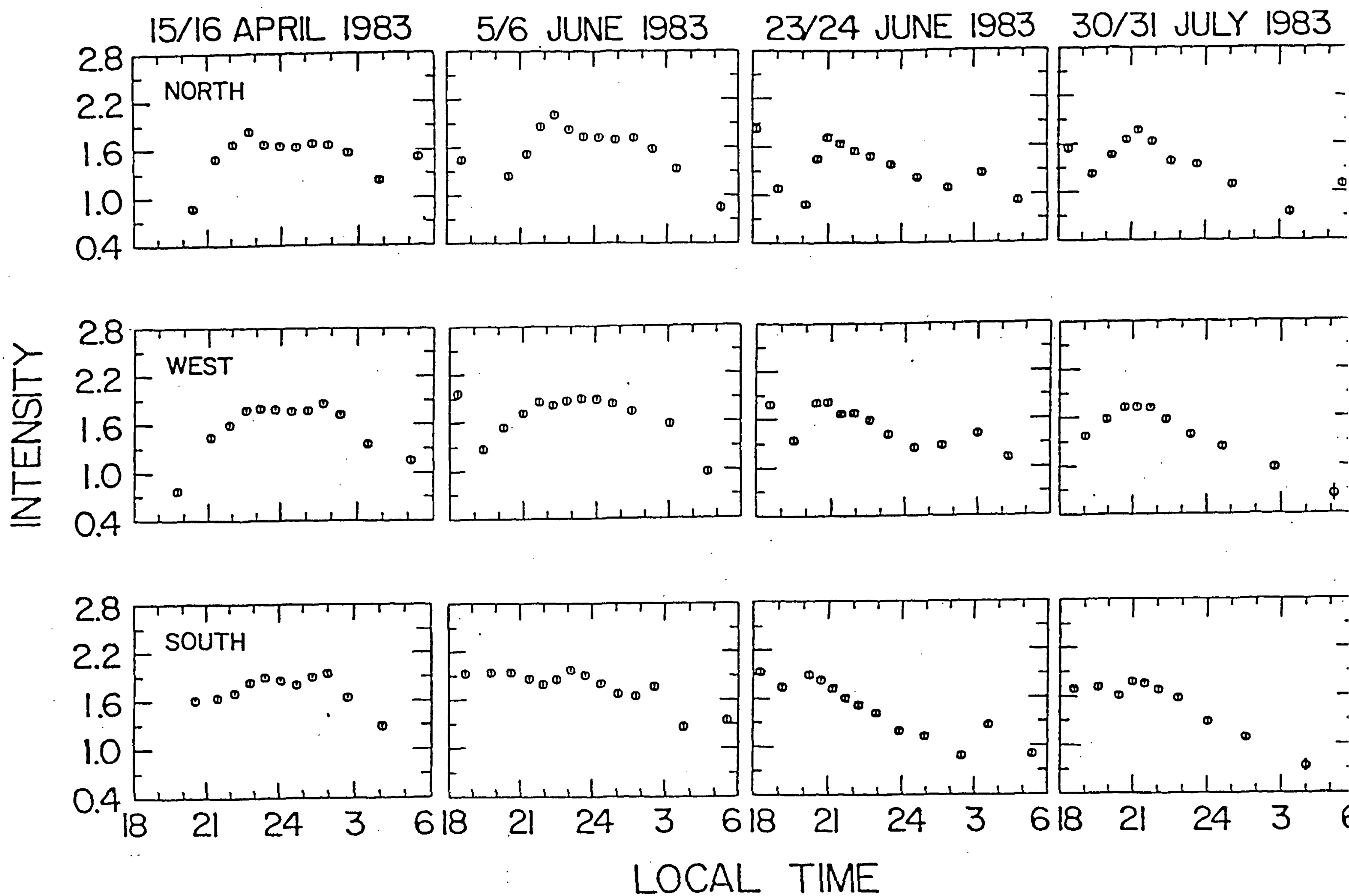

15/16 APRIL 1983
5/6 JUNE 1983
23/24 JUNE 1983
30/31 JULY 1983
NORTH
WEST
SOUTH
INTENSITY
2.8
2.2
1.6
1.0
0.4
18
21
24
3
6
LOCAL TIME

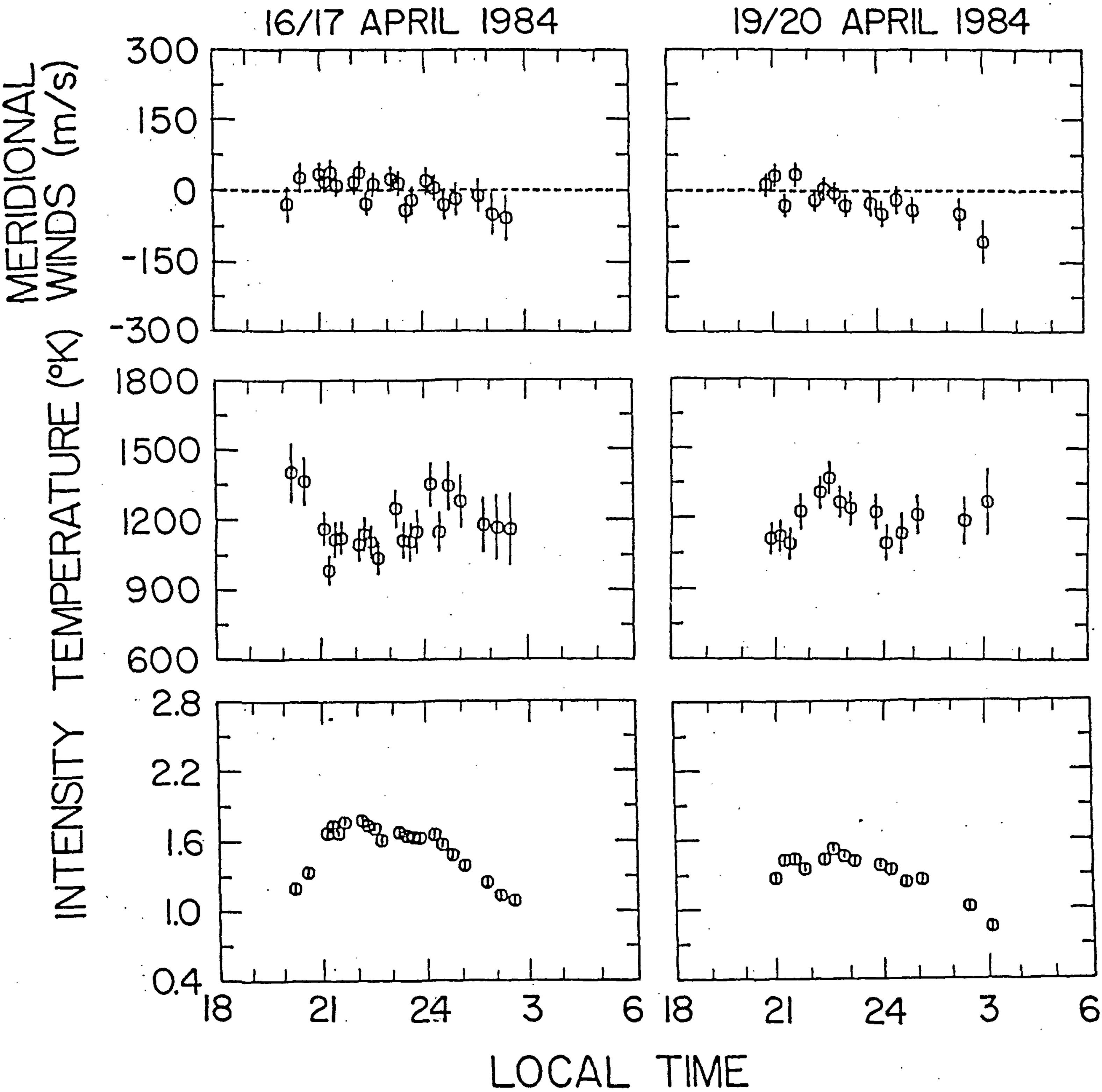
16/17 APRIL 1984
19/20 APRIL 1984
MERIDIONAL WINDS (m/s)
300
150
0
-150
-300
TEMPERATURE (°K)
1800
1500
1200
900
600
INTENSITY
2.8
2.2
1.6
1.0
0.4
18
21
24
3
6
LOCAL TIME

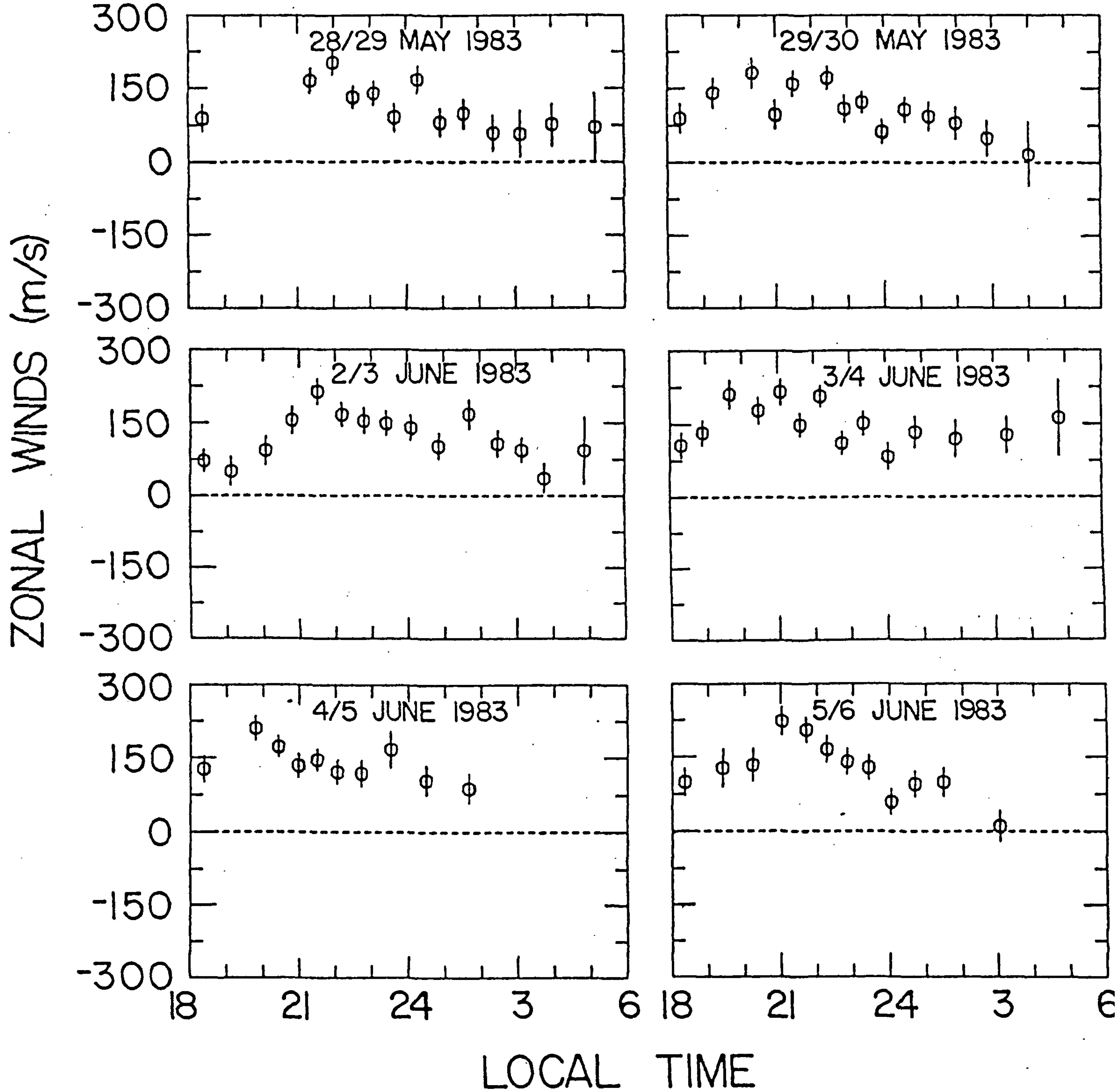

ZONAL WINDS (m/s)
300
150
0
-150
-300
28/29 MAY 1983
29/30 MAY 1983
2/3 JUNE 1983
3/4 JUNE 1983
4/5 JUNE 1983
5/6 JUNE 1983
18
21
24
3
6
LOCAL TIME

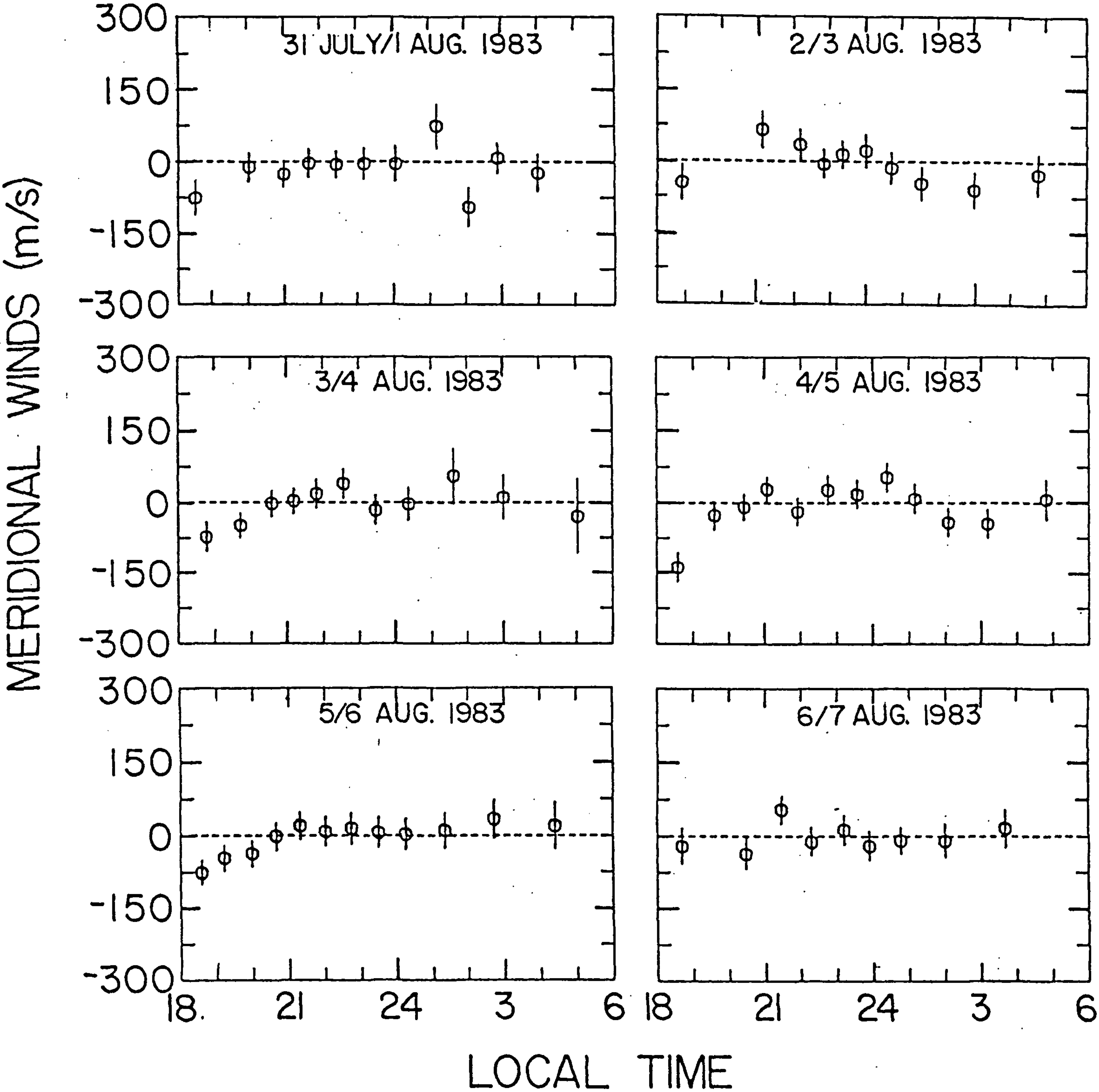
31 JULY/1 AUG. 1983
2/3 AUG. 1983
3/4 AUG. 1983
4/5 AUG. 1983
5/6 AUG. 1983
6/7 AUG. 1983
MERIDIONAL WINDS (m/s)
300
150
0
-150
-300
18
21
24
3
6
LOCAL TIME

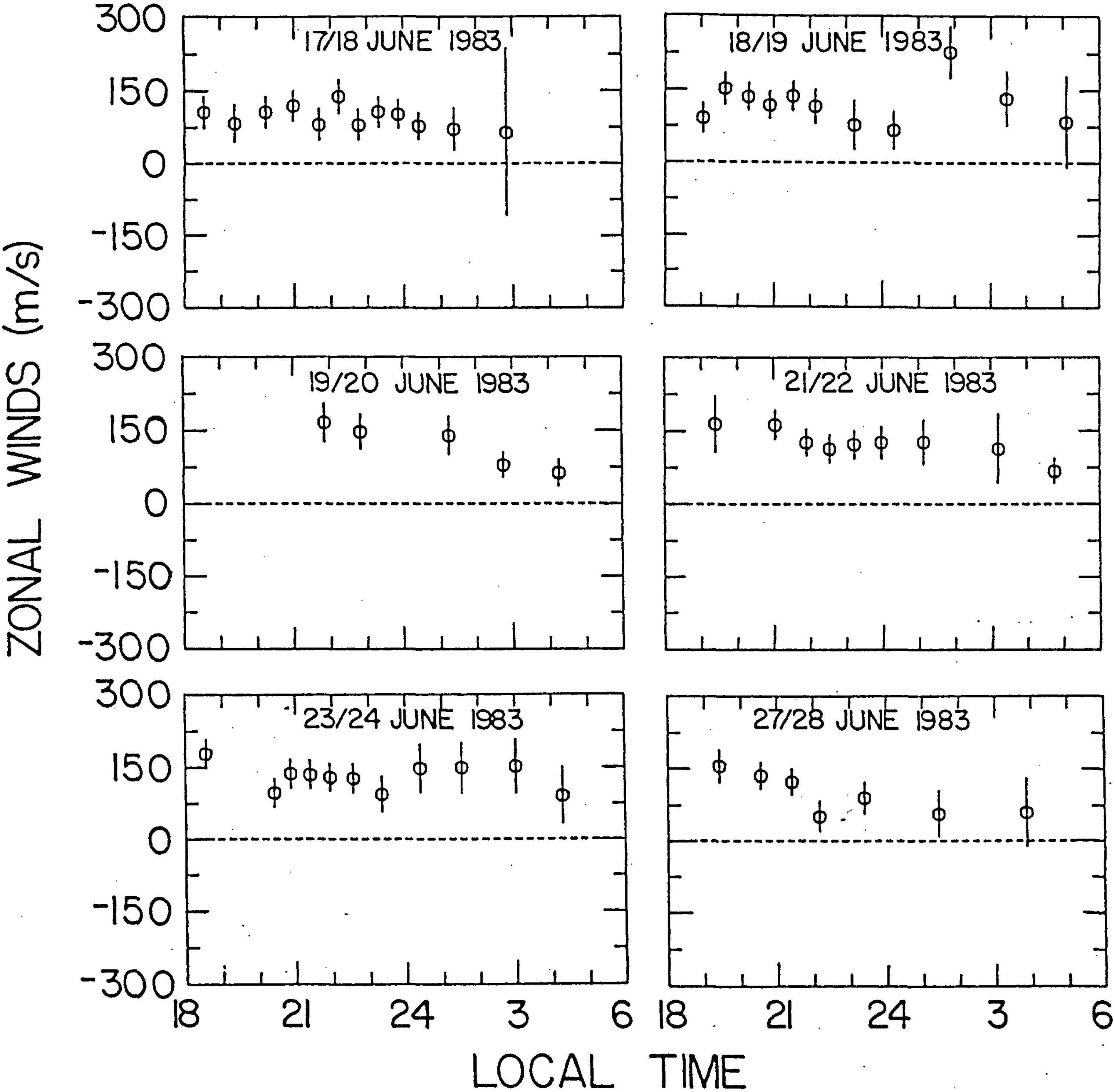

ZONAL WINDS (m/s)
300
150
0
-150
-300
17/18 JUNE 1983
18/19 JUNE 1983
19/20 JUNE 1983
21/22 JUNE 1983
23/24 JUNE 1983
27/28 JUNE 1983
18
21
24
3
6
LOCAL TIME

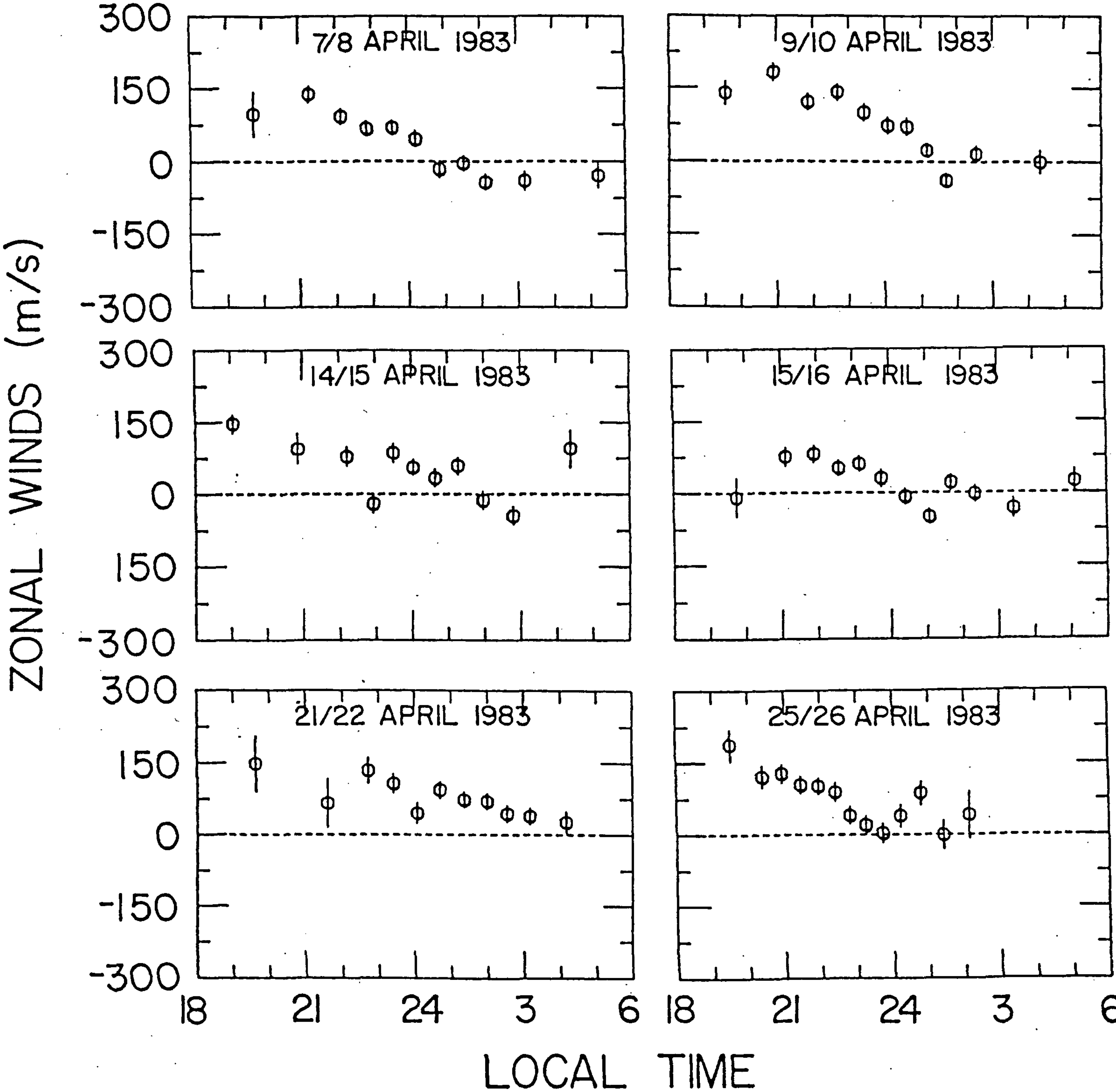
7/8 APRIL 1983
9/10 APRIL 1983
14/15 APRIL 1983
15/16 APRIL 1983
21/22 APRIL 1983
25/26 APRIL 1983
ZONAL WINDS (m/s)
300
150
0
-150
-300
18
21
24
3
6
LOCAL TIME

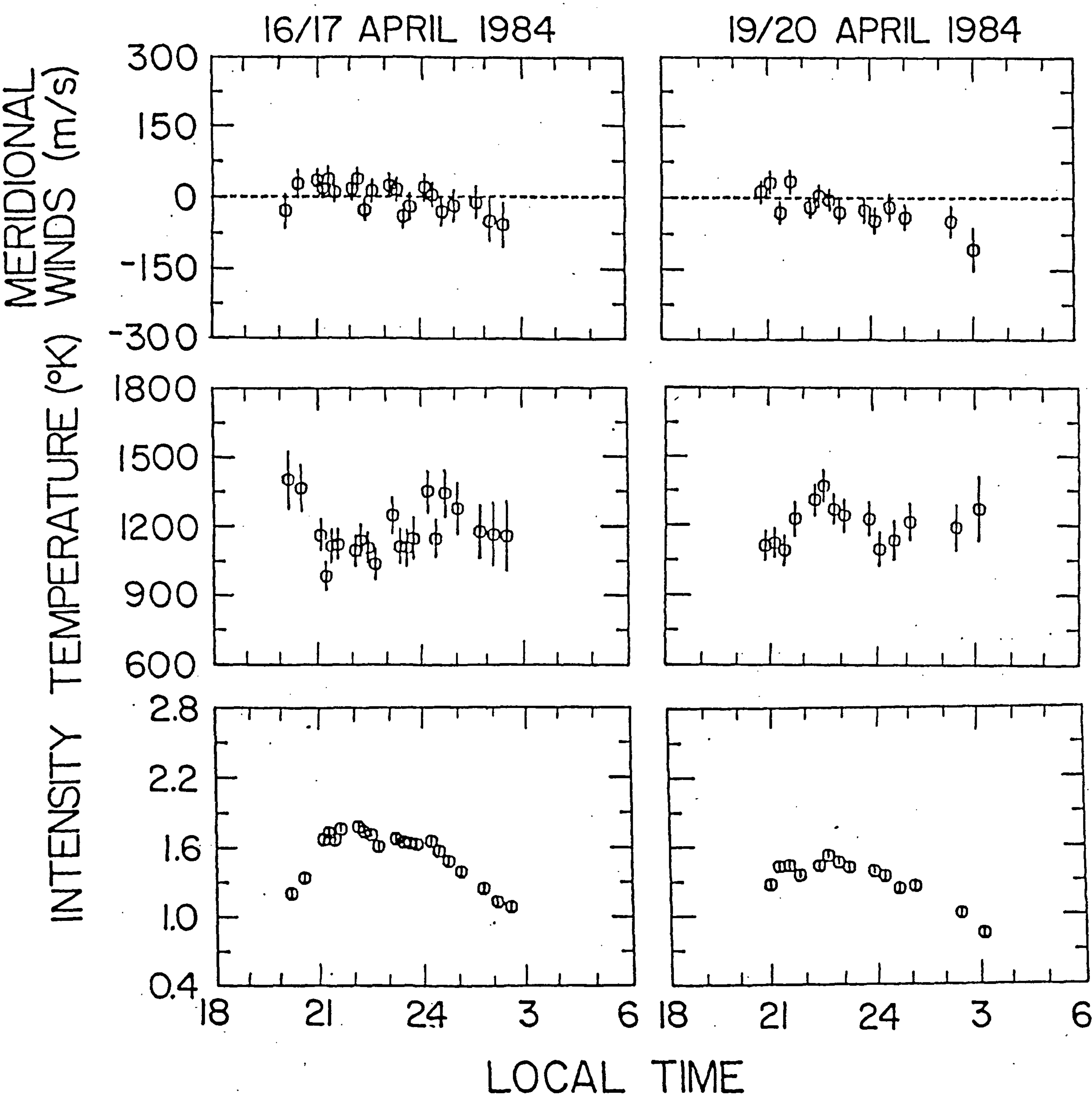
16/17 APRIL 1984
19/20 APRIL 1984
MERIDIONAL WINDS (m/s)
300
150
0
-150
-300
TEMPERATURE (°K)
1800
1500
1200
900
600
INTENSITY
2.8
2.2
1.6
1.0
0.4
18
21
24
3
6
LOCAL TIME

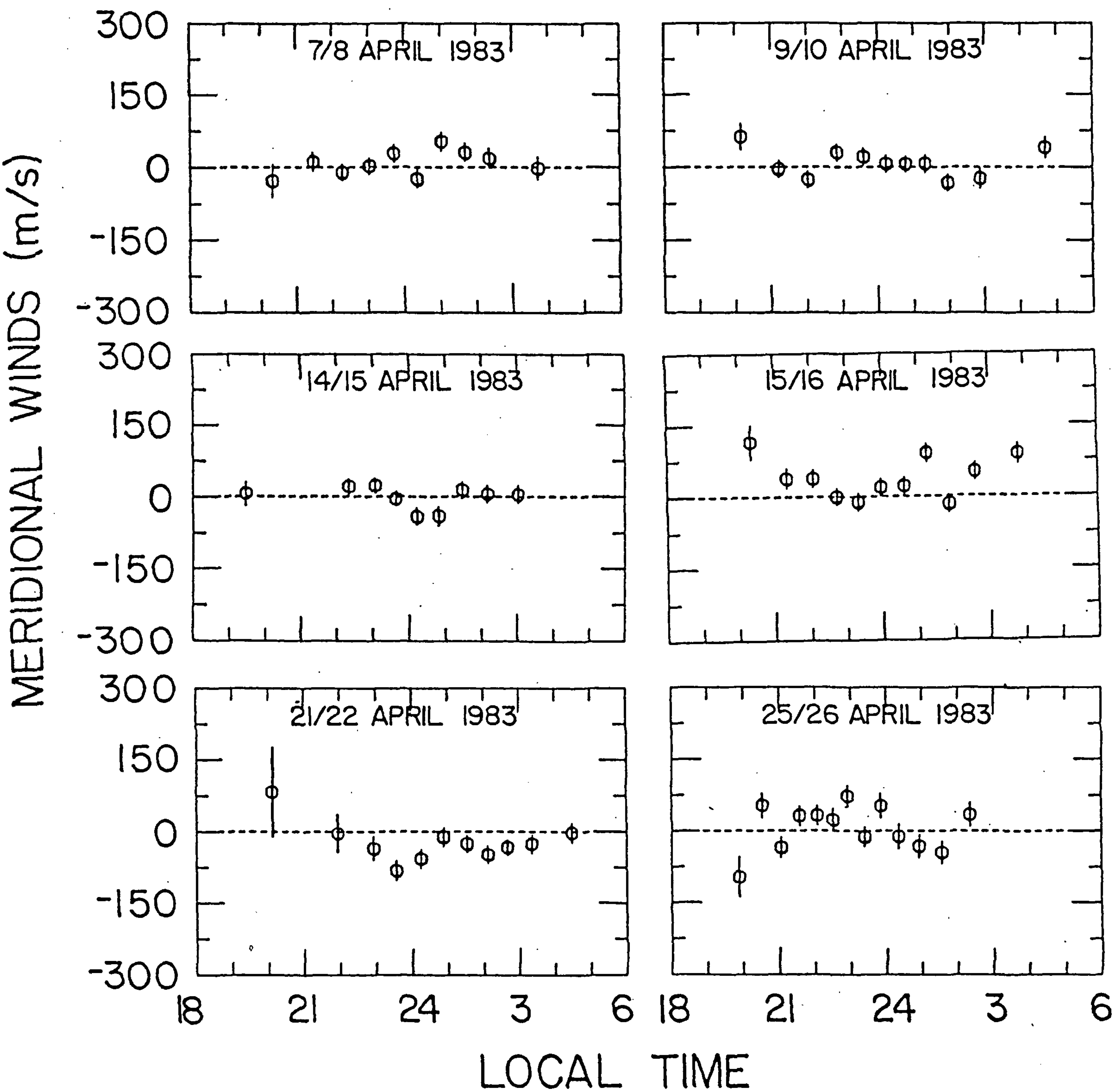

7/8 APRIL 1983
9/10 APRIL 1983
14/15 APRIL 1983
15/16 APRIL 1983
21/22 APRIL 1983
25/26 APRIL 1983
300
150
0
-150
-300
MERIDIONAL WINDS (m/s)
18
21
24
3
6
LOCAL TIME

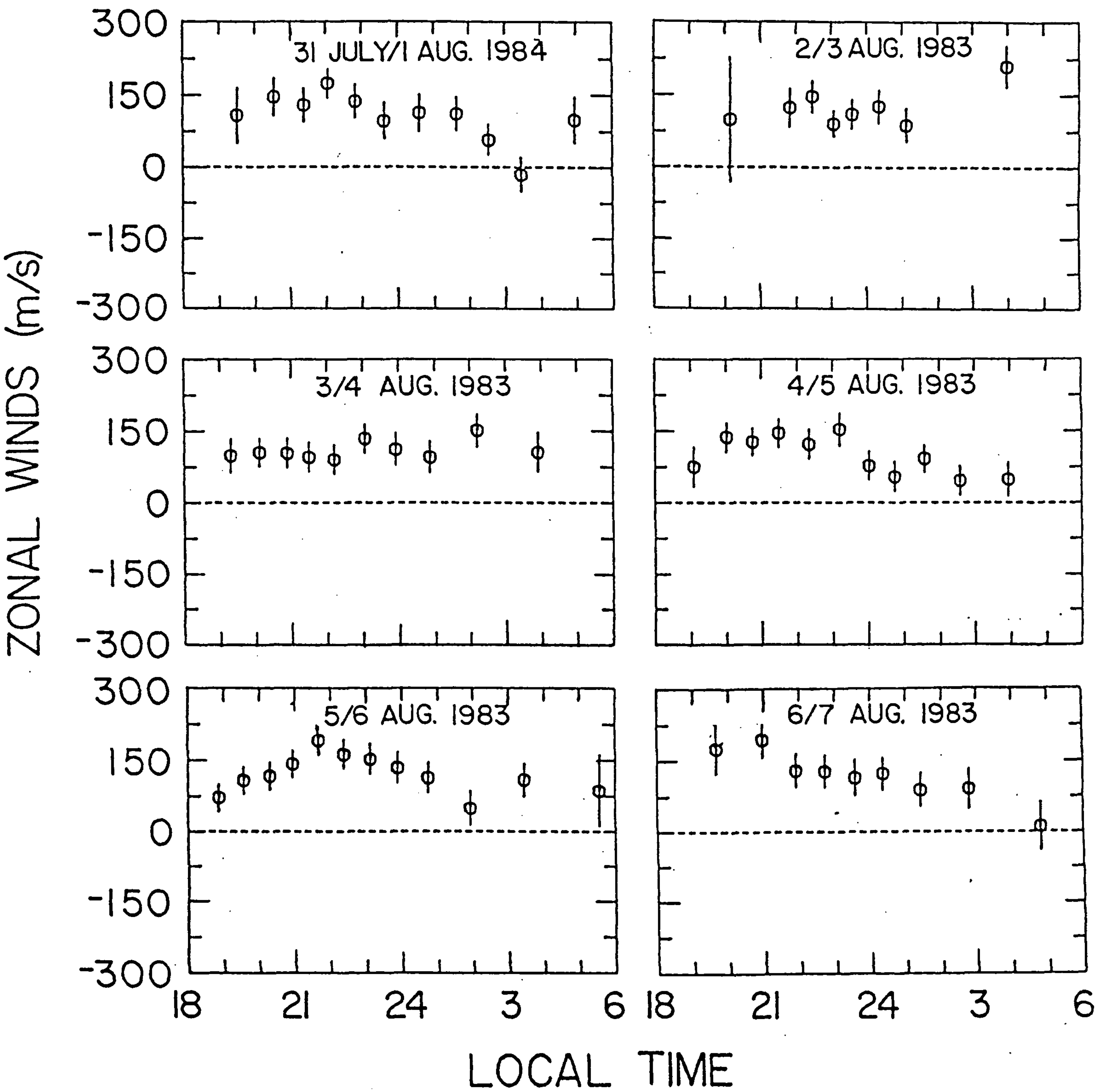

ZONAL WINDS (m/s)
300
150
0
-150
-300
31 JULY/1 AUG. 1984
2/3 AUG. 1983
3/4 AUG. 1983
4/5 AUG. 1983
5/6 AUG. 1983
6/7 AUG. 1983
18
21
24
3
6
LOCAL TIME

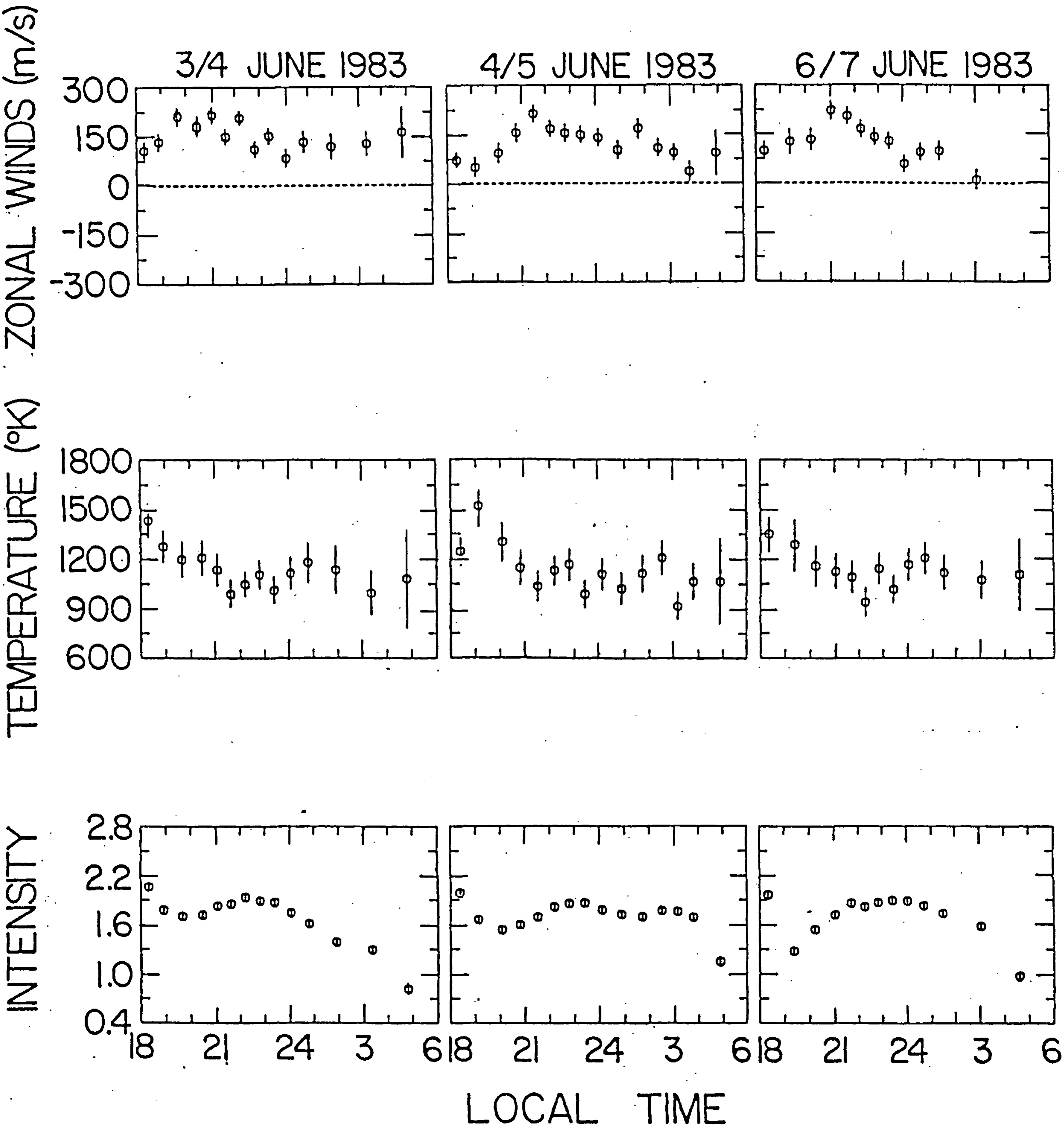

3/4 JUNE 1983
4/5 JUNE 1983
6/7 JUNE 1983
ZONAL WINDS (m/s)
300
150
0
-150
-300
TEMPERATURE (°K)
1800
1500
1200
900
600
INTENSITY
2.8
2.2
1.6
1.0
0.4
18
21
24
3
6
LOCAL TIME

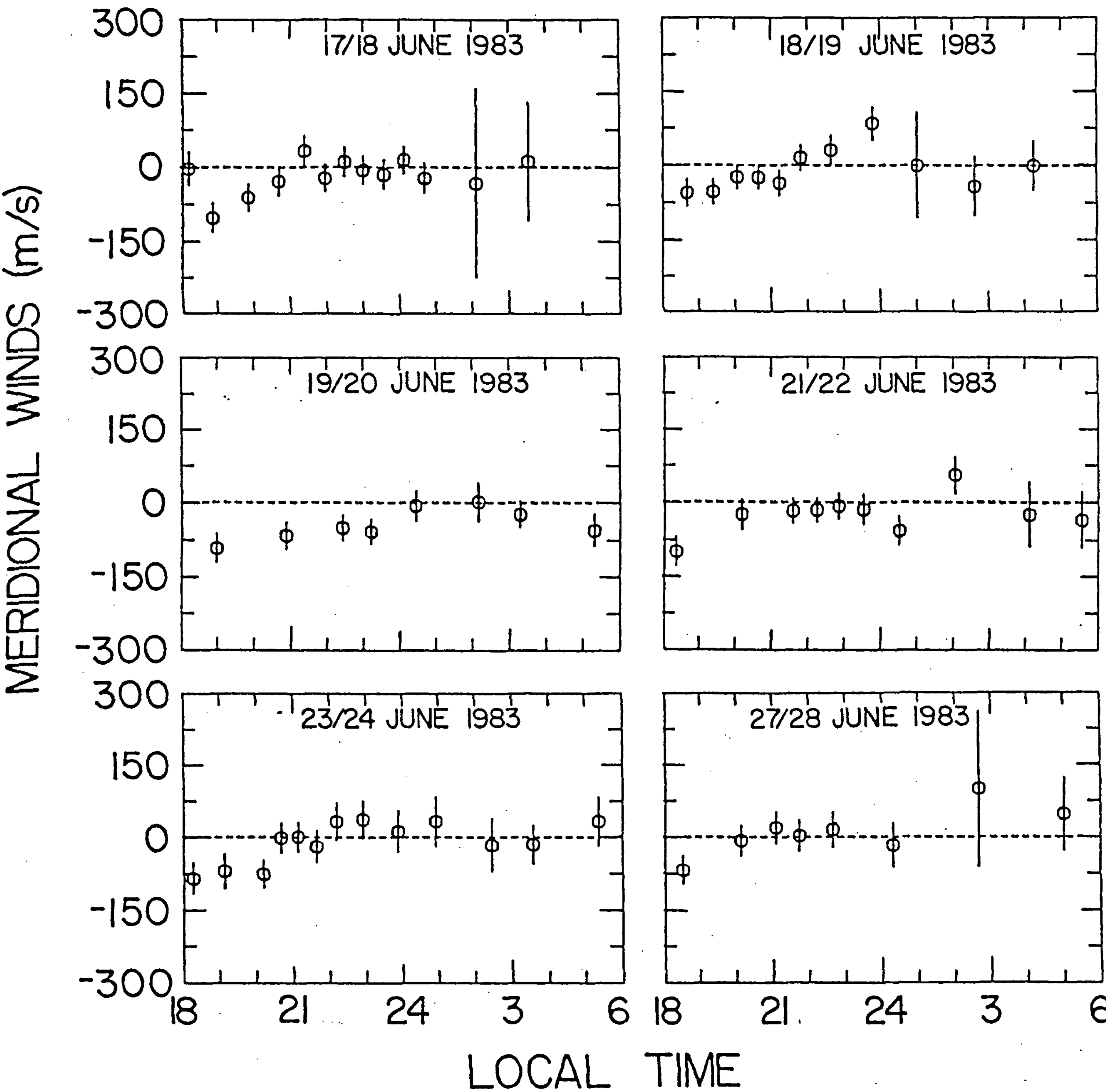
17/18 JUNE 1983
18/19 JUNE 1983
19/20 JUNE 1983
21/22 JUNE 1983
23/24 JUNE 1983
27/28 JUNE 1983
MERIDIONAL WINDS (m/s)
300
150
0
-150
-300
18
21
24
3
6
LOCAL TIME

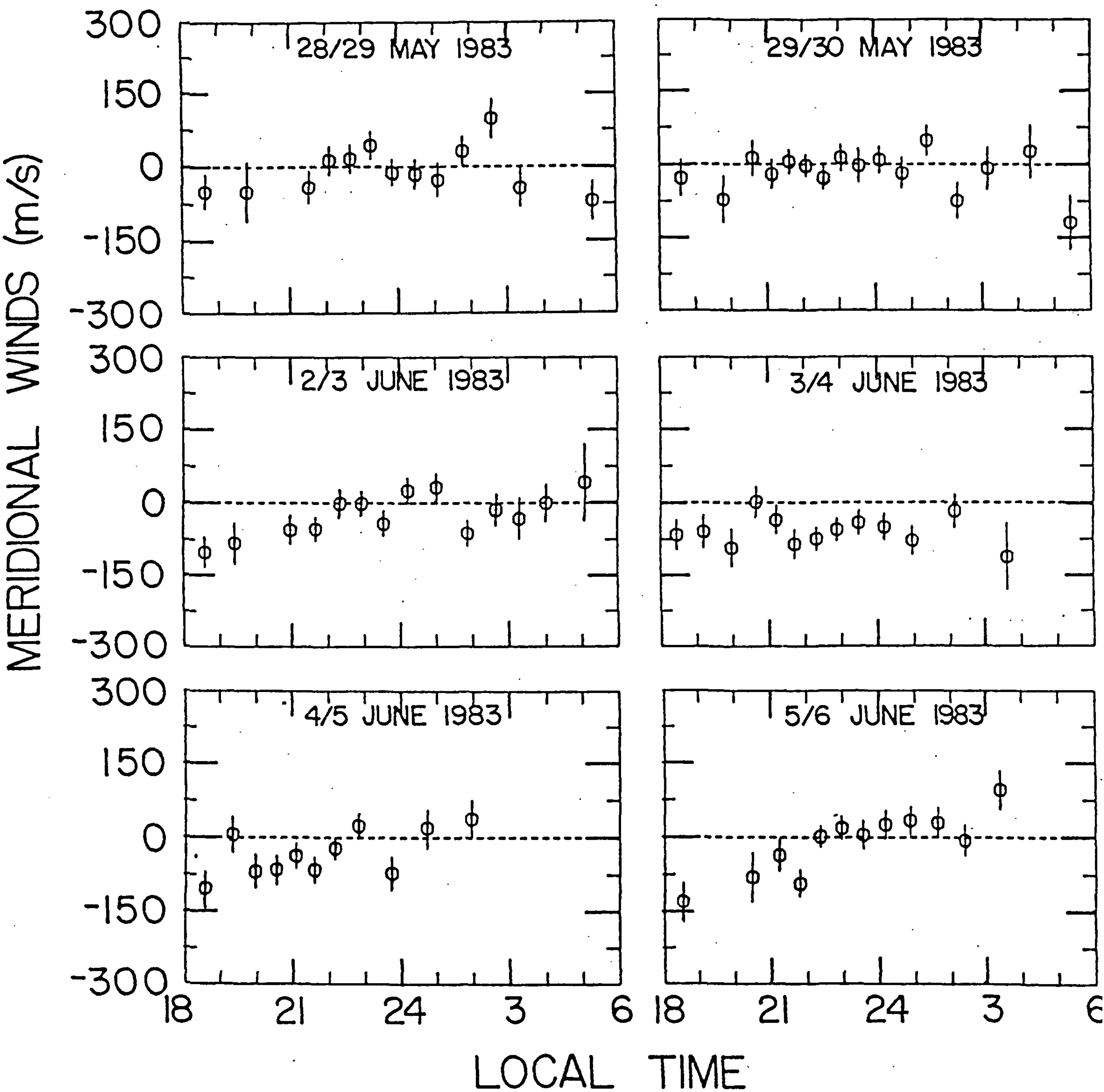
MERIDIONAL WINDS (m/s)
300
150
0
-150
-300
28/29 MAY 1983
29/30 MAY 1983
2/3 JUNE 1983
3/4 JUNE 1983
4/5 JUNE 1983
5/6 JUNE 1983
18
21
24
3
6
LOCAL TIME

Horizontal wind, temperature, and intensity observations
DAY 271, 1984
Arequipa, Peru

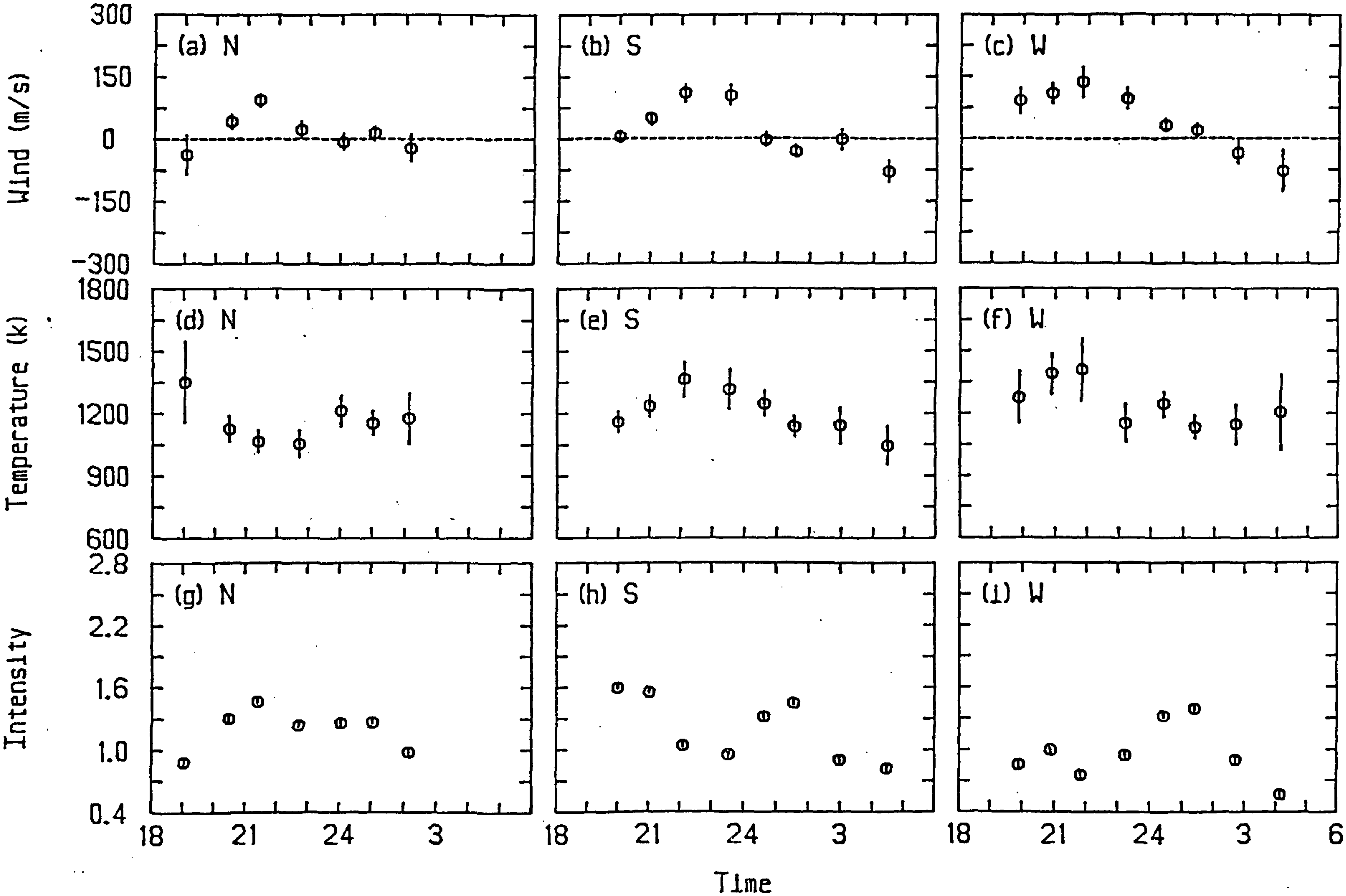

OCT 2, 1984

CONCLUSIONS

6300A surface brightnesses: Results

* Definite enhancement of 6300A surface brightness in the south as compared with other directions. Probably connected to the tropical airglow arcs. Meridional winds small (<25 m/s) throughout night.

* Indication of northward migration of the observed 6300A enhancement in the evening hours as observations approach local winter solstice. This is probably related to the observed poleward (to the south) meridional wind (of magnitude 50 m/s) in this period.

Equatorial thermospheric winds: Results

* Zonal component of winds always eastward, but speed approaches zero sooner near equinox than at summer solstice. Typical magnitude at peak is of order 100 to 150 m/s.

* Suggestion of zonal wind increase after twilight and recovery of 6300A emission for April data. Origin not clear but may be related to mid-night thermal enhancement.

* Meridional wind virtually zero for equinox in 1983; shows evening flow towards winter hemisphere in early evening for solstice data. Suggestion of post-midnight surge in April 1984 data.

* No major effects associated with mag. storm activity. Suggestion of decrease in zonal component below nominal levels.